Aust. J. Phys., 1984, **37**, 45–53

Atomic X-ray Transition Probabilities: A Comparison of the Dipole Length, Velocity and Acceleration Forms

H. M. Quiney[A] *and F. P. Larkins*[A,B]

[A] Department of Chemistry, Monash University, Clayton, Vic. 3168.
[B] Present address: Department of Chemistry, University of Tasmania, Hobart, Tas. 7001.

Abstract

The length, velocity and acceleration forms of the dipole transition operator are examined in calculations of diagram and satellite X-ray emission probabilities in the Ne^+ to Ar^{9+} isoelectronic series. All calculations are within the relaxed nonrelativistic Hartree–Fock framework, using separately optimized numerical wavefunctions for the initial and final electronic states. Divergence between the alternative forms of the transition moment, as the principal quantum number of the Rydberg electron and nuclear charge are increased, is discussed in the context of electron correlation differences between the initial and final states.

1. Introduction

The comparatively recent development of high resolution spectrometers to study X-ray emission from atoms and molecules has led to increased experimental activity in this field at a fundamental level (Ågren *et al.* 1978; Nordgren *et al.* 1979; Nordling 1982). X-ray emission has also become a widely used analytical technique for probing solid systems (Best 1974), and for diagnosing the consequences of heavy ion–atom collisions, often involving multiply ionized atomic systems (Larkins 1971).

Previous calculations of X-ray transition probabilities for atoms have been restricted mainly to diagram lines using the length form of the dipole operator. In the present paper, oscillator strengths for X-ray diagram and some satellite transitions are evaluated using the length, velocity and acceleration forms of the dipole transition matrix element. Such a detailed comparison has not previously been made at the relaxed Hartree–Fock (HF) level, although Cohen and MacEachran (1972) have evaluated oscillator strengths for the isoelectronic sequence at the frozen HF level in the alternative length and velocity forms. Much formal discussion has also taken place (see Hansen 1967; Starace 1971, 1973; Grant 1974; Grant and Starace 1975) examining the relative merits of the three formulations employing approximate wavefunctions, but without resolution of the problem.

2. Theoretical Considerations

High resolution X-ray emission spectra (XES) of free atomic systems are usually complex, having a series of satellite lines as well as the diagram lines. The challenge is to calculate both the energies and intensities of these lines to high accuracy.

0004-9506/84/010045$02.00

If the initial atomic state of the ionized system with energy E_n^{i} is represented by the atomic state function (ASF) $\Phi_n^{\mathrm{i}}(N-1)$, and the final atomic state with energy E_m^{f} is represented by the ASF $\Phi_m^{\mathrm{f}}(N-1)$, then the X-ray energies for diagram and satellite lines are given (in atomic units) by

$$E_{mn} = h\nu_{mn} = E_n^{\mathrm{i}} - E_m^{\mathrm{f}}, \tag{1}$$

and the transition probability, derived by time-dependent perturbation theory, is given by

$$A_{mn} = (64\pi^4 \nu_{mn}^3 / 3hc^3) |\, M_{mn}\,|^2, \tag{2}$$

where M_{mn} is the transition matrix element connecting states m and n. Within the dipole approximation we have

$$M_{mn} = \langle \Phi_m^{\mathrm{f}} \,|\, \sum_{\mu} \boldsymbol{d}_{\mu} \,|\, \Phi_n^{\mathrm{i}} \rangle, \tag{3}$$

where $\boldsymbol{d}_{\mu}$ is the formal single-particle dipole operator. Application of the off-diagonal hypervirial theorem (Manson 1976) with the exact eigenfunctions of a single Hamiltonian yields three formally equivalent expressions for $\boldsymbol{d}_{\mu}$:

$$\boldsymbol{d}_{\mu} = \boldsymbol{r}_{\mu} \tag{4a}$$

$$= (1/E_{mn}) \nabla_{\mu} \tag{4b}$$

$$= (1/E_{mn}^2) Z_j \boldsymbol{r}_j / |\, \boldsymbol{r}_j \,|^3 ; \tag{4c}$$

these are known respectively as the length, velocity and acceleration forms of the dipole operator. In equations (4) $\boldsymbol{r}_{\mu}$ is the position operator, ∇_{μ} is the gradient operator associated with electron μ, Z_j is the nuclear charge, and $\boldsymbol{r}_j$ is the position vector of electron μ in the coordinates centred on the nucleus j. The acceleration form of $\boldsymbol{d}_{\mu}$ must be regarded as approximate, as it neglects all inter-electron repulsion effects in the transition moment, and includes only contributions from the nuclear Coulomb field in the atomic potential.

The use of relaxed HF wavefunctions to describe the electronic states destroys the necessary equivalence of the forms and, as was noted by Cohen and MacEachran (1972), the off-diagonal hypervirial theorem must be replaced by the more general form

$$\begin{aligned}(E^{\mathrm{f}} - E^{\mathrm{i}}) \langle \Phi_{\mathrm{f}} \,|\, A \,|\, \Phi_{\mathrm{i}} \rangle &= \langle \Phi_{\mathrm{f}} \,|\, [A, H] \,|\, \Phi_{\mathrm{i}} \rangle \\ &\quad + \langle \Phi_{\mathrm{f}} \,|\, A(H - H_{\mathrm{f}}) - (H - H_{\mathrm{i}}) A \,|\, \Phi_{\mathrm{i}} \rangle, \end{aligned} \tag{5}$$

where A is any Hermitian operator, H is a single Hamiltonian operator, and Φ_{i}, Φ_{f}, H_{i} and H_{f} are defined by the relations

$$H_{\mathrm{i}} \,|\, \Phi_{\mathrm{i}} \rangle = E_{\mathrm{i}} \,|\, \Phi_{\mathrm{i}} \rangle, \qquad H_{\mathrm{f}} \,|\, \Phi_{\mathrm{f}} \rangle = E_{\mathrm{f}} \,|\, \Phi_{\mathrm{f}} \rangle. \tag{6a, b}$$

In this study, the oscillator strengths associated with diagram and selected satellite X-ray emission lines for the Ne^+ isoelectronic series $Z = 10$–18 were investigated,

and the processes chosen as being representative of classes of transitions frequently associated with 'shake up' states in XES were the following:

A, $1s^1 2s^2 2p^6(^2S) \rightarrow 1s^2 2s^2 2p^5(^2P)$;

B, $1s^1 2s^2 2p^5(^3P)np(^2S) \rightarrow 1s^2 2s^2 2p^5(^2P)$, $n = 3, 4, 5, 6$;

C, $1s^1 2s^2 2p^6(^2S) \rightarrow 1s^2 2s^2 2p^4(^1D, ^1S, ^3P)3p(^2P)$;

D, $1s^1 2s^2 2p^5(^1P)3p(^2S) \rightarrow 1s^2 2s^2 2p^4(^1D, ^1S, ^3P)3p(^2P)$.

All calculations were performed at the relaxed nonrelativistic HF level, using separately optimized initial and final state wavefunctions. The program of Mayers and O'Brien (1968), modified as described in previous work (see Dyall and Larkins 1982), was used to evaluate the orbital wavefunctions and the total state energies. The transition moment expressions are given in Table 1 following Dyall (1980). The determinants of overlap and dipole integrals result from the inclusion of orbital relaxation effects, and may be found by application of Löwdin's (1955) treatment of the non-orthogonality problem.

Table 1. Matrix element expressions for various diagram and satellite X-ray emission processes for relaxed HF wavefunctions

Here S and P represent $\det|\langle 1s|1s\rangle\langle 2s|2s\rangle|$ and $\langle 2p|2p\rangle$ respectively. Determinants are represented by diagonal terms only; each determinant containing the dipole operator d consists of a sum of such terms, in which the operator is included in each row in turn. The notation [ ] represents an orbital vacancy in the electron configuration: for example,

$$[1s2p(^3P)]3p \equiv 1s^1 2s^2 2p^5(^3P)3p$$

Process	Initial state	Final state	Expression
A	[1s]	[2p]	$\sqrt{2}/\sqrt{3}\det\|\langle 2p\|d\|1s\rangle\langle 2s\|2s\rangle\|\,SP^5$
B	$[1s2p(^3P)]np$	[2p]	$1/\sqrt{3}\det\|\langle np\|d\|1s\rangle\langle 2s\|2s\rangle\|\,SP^5$
C	[1s]	$[2p^2(^1D)]3p$	$-\frac{1}{3}\sqrt{10}\det\|\langle 2p\|d\|1s\rangle\langle 2s\|2s\rangle\|\langle 2p\|np\rangle\,SP^5$
		$[2p^2(^3P)]3p$	$-\sqrt{2}\det\|\langle 2p\|d\|1s\rangle\langle 2s\|2s\rangle\|\langle 2p\|np\rangle\,SP^4$
		$[2p^2(^1S)]3p$	$-\sqrt{2}/\sqrt{3}\det\|\langle 2p\|d\|1s\rangle\langle 2s\|2s\rangle\|\langle 2p\|np\rangle\,SP^4$
D	$[1s2p(^1P)]np$	$[2p^2(^1D)]3p$	$2/\sqrt{15}$
		$[2p^2(^3P)]3p$	0 } $\det\|\langle 2p\|d\|1s\rangle\langle 2s\|2s\rangle\|\langle np\|np\rangle\,SP^4$
		$[2p^2(^1S)]3p$	$-2/3\sqrt{3}$
		$+[2p^2(^1D)]3p$	$4/3\sqrt{15}$
		$[2p^2(^3P)]3p$	$2/\sqrt{3}$ } $\det\|\langle 2p\|d\|1s\rangle\langle 2s\|2s\rangle\|\langle 2p\|np\rangle\langle np\|2p\rangle\,SP^3$
		$[2p^2(^1S)]3p$	0
		$+[2p^2(^1D)]3p$	$-5/3\sqrt{15}$
		$[2p^2(^3P)]3p$	$-1/\sqrt{3}$ } $\det\|\langle np\|d\|1s\rangle\langle 2s\|2s\rangle\|\langle 2p\|np\rangle\,SP^4$
		$[2p^2(^1S)]3p$	$1/3\sqrt{3}$

The dominant contributions to the transition probability for any of the processes may be found by examination of the matrix element expressions in Table 1, and may be interpreted in a simple independent particle sense. Transition A is the diagram line and may be viewed as a $2p \rightarrow 1s$ dipole transition. Similarly, transitions of class B correspond to high energy satellites involving an $np \rightarrow 1s$ dipole transition.

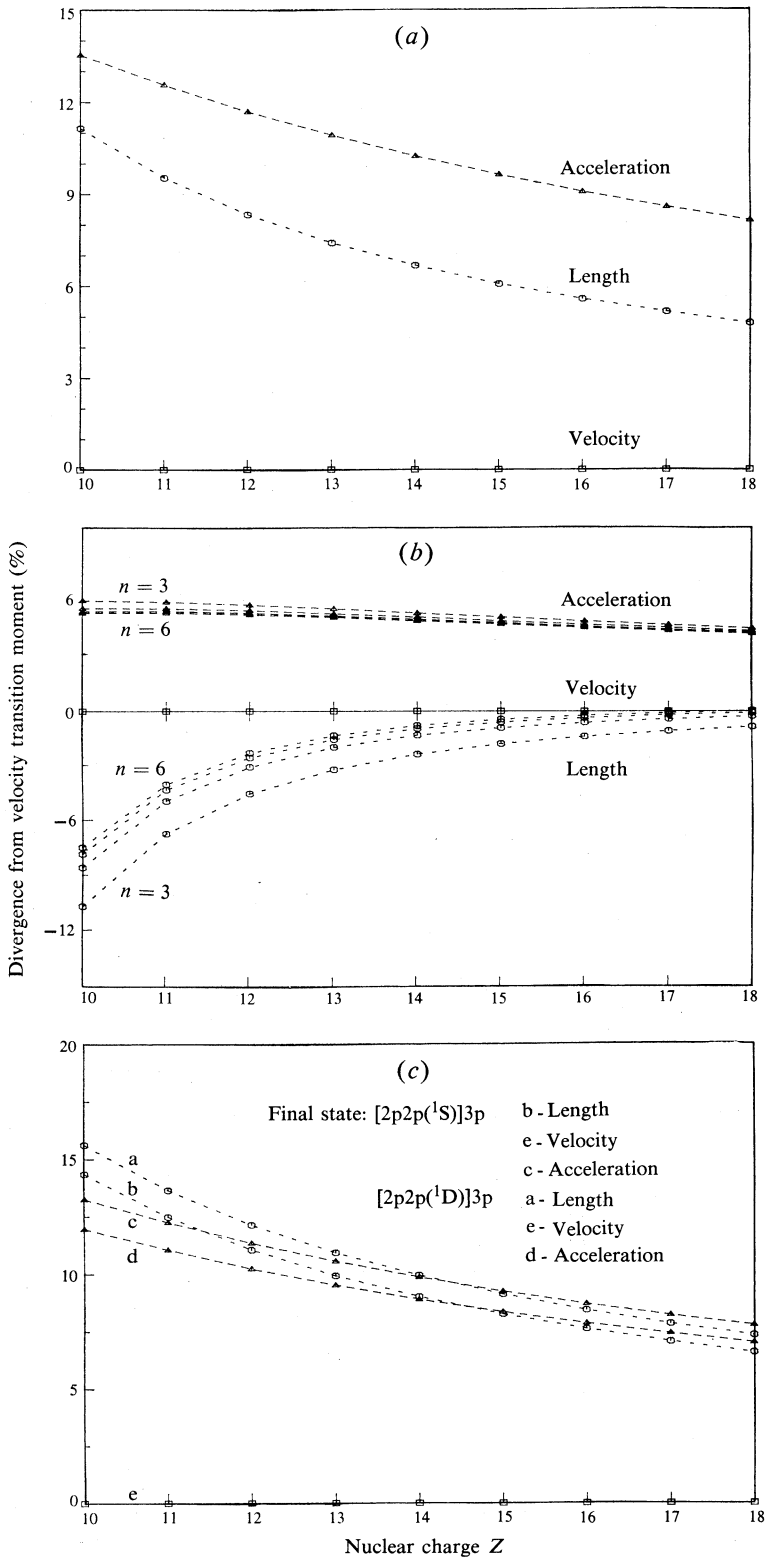
(a)
Acceleration
Length
Velocity
(b)
n = 3
n = 6
Acceleration
Velocity
n = 6
Length
n = 3
Divergence from velocity transition moment (%)
(c)
Final state: [2p2p(1S)]3p
b - Length
e - Velocity
c - Acceleration
[2p2p(1D)]3p
a - Length
e - Velocity
d - Acceleration
a
b
c
d
e
Nuclear charge Z

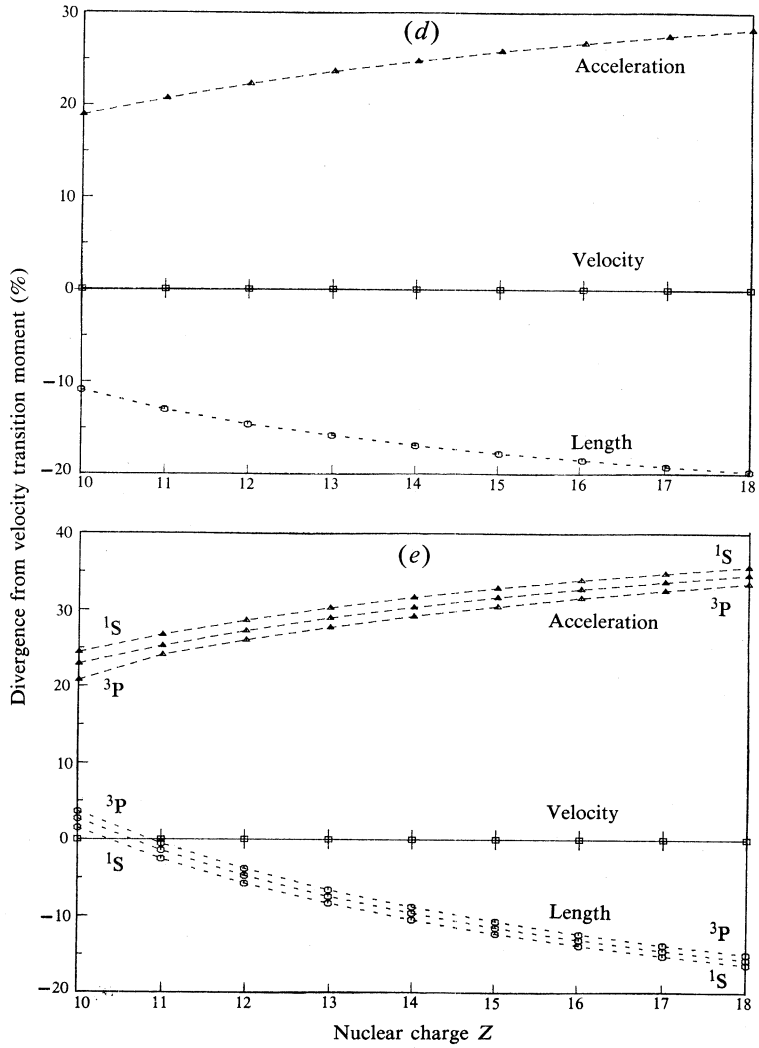

Fig. 1. Divergence of the length and the acceleration transition moments from the velocity transition moment (see equation 7) for the following lines of the neon isoelectronic series:

(*a*) the diagram line [1s] → [2p];

(*b*) the [1s2p(^{3}P)]*n*p → 2p] initial state correlation satellites;

(*c*) the [1s2p(^{1}P)]3p → [2p2p(^{1}S, ^{1}D)]3p multiply excited correlation satellites;

(*d*) the [1s2p(^{1}P)]3p → [2p2p(^{3}P)]3p multiply excited correlation satellite line;

(*e*) the [1s] → [2p2p(^{1}D, ^{1}S, ^{3}P)]3p final state correlation satellites.

Transitions in class C correspond to a two electron process, involving a 2p → 1s dipole 'shake-down' coupled with a 2p → *n*p monopole 'shake-up'. Matrix elements for process D include terms representing direct 2p → 1s dipole transitions, as well as cooperative *n*p → 1s and 2p → *n*p transitions. The above analysis is, of course, purely designed to provide some insight into these processes at an independent particle level. A more complete quantum-mechanical treatment requires that the

radiative transition occurs between the many electron initial and final ion states. Following Dyall and Larkins (1982), class B transitions are initial state correlation or Rydberg participator satellites, class C transitions are final state correlation satellites and class D transitions are multiply excited correlation satellites.

3. Results and Discussion

The equivalence of the length, velocity and acceleration forms is a necessary (but not sufficient) condition for exactness of the final calculated transition moment. Accurate experimental values of transition probabilities for the systems studied are available for only a few of the neon lines, and then only as values relative to the diagram line. The increased experimental activity in the field is likely to provide more detailed information to assess the accuracy of relaxed HF calculations of both energies and intensities. The purpose of this paper is to examine the mathematical and physical relationships between the alternative forms of the transition moment within a relaxed HF framework.

Divergence between the forms is determined by

(*a*) the importance of the second term in equation (5);

(*b*) the accuracy of the solutions to the HF equations.

For numerical atomic calculations we may reasonably assume (*b*) to be of negligible importance, so from equation (5), equivalence of two forms suggests that the initial and final states are described by a single Hamiltonian operator H, such that $H_i \approx H$ and $H_f \approx H$. The divergence between the alternative forms of $|M_{if}|^2$ is presented for the examined processes as a percentage difference from the velocity form:

$$\text{divergence } (\%) = \{|M_{if}(d)|^2 - |M_{if}(v)|^2\}/|M_{if}(v)|^2, \tag{7}$$

where $|M_{if}(d)|$ is the transition moment in the formulation d, where d may be the length, velocity or acceleration (l, v or a) representation.

For the diagram line in Fig. 1*a* systematic convergence is observed as the nuclear charge Z is increased from 10 to 18. This may be explained by noting that as Z is increased, the central Coulomb field tends to dominate over electron repulsion effects, and the initial and final state Hamiltonians tend toward a single hydrogenic form. This fulfils the essential condition for equivalence, diminishing the troublesome term in equation (5). This tendency towards equivalence should not be interpreted as a suggestion that relaxed HF transition probabilities become more reliable for the highly charged ions of large nuclear charge. The values converge toward one another, but all neglect the strong correlation contribution expected for the core levels, and the onset of non-negligible relativistic effects in these systems. The good agreement between the length and velocity forms (5–11 %) is evidence that the electron correlation contributions, which are ignored at the HF level, are not too different in the initial and final state representations.

The acceleration values converge more slowly on the other forms because of the approximate nature of the acceleration dipole operator which, as previously discussed, ignores the inter-electron terms in the HF potential functions. The numerical values for the velocity form are given in Table 2. The corresponding values for the length and acceleration forms may be determined from Fig. 1*a*.

The Rydberg participator transitions also exhibit this convergent behaviour with increasing Z, and also with increasing principal quantum number n (see Fig. 1*b*).

Table 2. Relaxed HF values of the transition moments for the X-ray diagram and final state correlation satellite lines of the neon isoelectronic series

Velocity form is $|M_{if}(v)|^2$

Element	Transition			
	[1s]–[2p]	[1s]–[2p²(¹S)]3p	[1s]–[2p²(¹D)]3p	[1s]–[2p²(³P)]3p
Ne^{+}	6·58(−3)	2·36(−8)	8·17(−6)	3·73(−6)
Na^{2+}	5·90(−3)	1·29(−9)	5·55(−6)	1·55(−6)
Mg^{3+}	5·26(−3)	1·81(−8)	3·58(−6)	6·28(−7)
Al^{4+}	4·70(−3)	3·28(−8)	2·33(−6)	2·54(−7)
Si^{5+}	4·21(−3)	3·99(−8)	1·54(−6)	1·02(−7)
P^{6+}	3·78(−3)	4·13(−8)	1·05(−6)	4·02(−8)
S^{7+}	3·40(−3)	3·97(−8)	7·37(−7)	1·43(−8)
Cl^{8+}	3·08(−3)	3·65(−8)	5·29(−7)	4·26(−8)
Ar^{9+}	2·79(−3)	3·28(−8)	3·88(−7)	8·01(−9)

Table 3. Relaxed HF values of the transition moments for the [1s2p(³P)]*n*p → [2p] initial state correlation satellites of the neon isoelectronic series

Velocity form is $|M_{if}(v)|^2$

Element	Transition [1s2p(³P)]*n*p–[2p]			
	3p	4p	5p	6p
Ne^{+}	2·60(−5)	1·05(−5)	5·09(−6)	2·83(−6)
Na^{2+}	4·94(−5)	2·09(−5)	1·04(−5)	5·87(−6)
Mg^{3+}	6·99(−5)	3·03(−5)	1·52(−5)	8·65(−6)
Al^{4+}	8·54(−5)	3·73(−5)	1·88(−5)	1·07(−5)
Si^{5+}	9·60(−5)	4·18(−5)	2·11(−5)	1·20(−5)
P^{6+}	1·02(−4)	4·43(−5)	2·24(−5)	1·27(−5)
S^{7+}	1·05(−4)	4·53(−5)	2·28(−5)	1·30(−5)
Cl^{8+}	1·06(−4)	4·52(−5)	2·27(−5)	1·29(−5)
Ar^{9+}	1·05(−4)	4·44(−5)	2·22(−5)	1·26(−5)

Table 4. Relaxed HF values of the transition moments for the multiply excited correlation satellite lines of the neon isoelectronic series

Velocity form is $|M_{if}(v)|^2$

Element	Transition [1s2p(¹P)]3p–[2p²(*L*)]3p for ^{2s+1}L		
	¹D	³P	¹S
Ne^{+}	2·85(−3)	2·78(−7)	1·59(−3)
Na^{2+}	2·51(−3)	4·13(−7)	1·40(−3)
Mg^{3+}	2·21(−3)	4·34(−7)	1·23(−3)
Al^{4+}	1·95(−3)	3·98(−7)	1·09(−3)
Si^{5+}	1·74(−3)	3·43(−7)	9·69(−4)
P^{6+}	1·55(−3)	2·87(−7)	8·65(−4)
S^{7+}	1·39(−3)	2·38(−7)	7·77(−4)
Cl^{8+}	1·25(−3)	1·96(−7)	7·00(−4)
Ar^{9+}	1·14(−3)	1·62(−7)	6·34(−4)

Examination of Table 1 reveals that these, and the diagram transition, are essentially $np \rightarrow 1s$ dipole transitions, considered in simple one electron terms. Increasing n has the effect of causing the Rydberg orbital to become more strictly hydrogenic, and diminishing the contribution to the second term of equation (5). Agreement between the length and velocity forms for these processes ranges from 0–11%, with rather slower convergence for the acceleration form. The numerical values of the velocity form for the various n values are presented in Table 3.

Of the remaining cases considered, only two cases exhibit convergent behaviour (see Fig. 1*c*), namely the ^1S and ^1D final core-state terms of process D. Table 1 reveals these to be dominated by the dipole $2p \rightarrow 1s$ transition, with only minor $np \rightarrow 1s$ and $2p \rightarrow np$ cooperative contributions. The ^3P final state process has no dipole $2p \rightarrow 1s$ contribution, with the most substantial part of the moment arising from the $np \rightarrow 1s$ transition. The probability of this process is largely determined by the $\langle 2p \,|\, np \rangle$ overlap integral, which is of the approximate order 10^{-3}–10^{-4}. The divergent nature of the alternative transition moments with increasing Z (see Fig. 1*d*) suggests that the correlation contributions in the initial and final state Hamiltonians are no longer similar, and when applied to equation (5) lead to non-negligible differences between the forms. In the independent particle model this may be understood by noting that the initial and final state np orbitals are constructed in very different HF potentials (based on simple screening considerations), leading to divergence between transition moments which involve the Rydberg electron. The numerical values of the velocity form for the multiply excited correlation satellites are presented in Table 4.

The processes C all exhibit strongly divergent behaviour (see Fig. 1*e*), and like the ^3P final state term considered above, may be interpreted as involving states which involve significantly different correlation contributions. In the light of the convergent diagram line calculations, this correlation difference would seem to be most significant when we consider transitions involving valence and Rydberg electrons, such as the divergent member of class D and all the processes of class C. The numerical values of the velocity form for these satellites are given in Table 1.

In general, the convergent processes are all described, in single particle terms, by dipole $np \rightarrow 1s$ transitions alone.

It is concluded from the transition moment data in Tables 2–4 and the calculated transition energies* that the transition probabilities for the diagram and the ^1D and ^1S multiply excited satellite transitions are of a similar order of magnitude. The initial state correlation satellite lines have probabilities at least an order of magnitude lower, while the final state correlation satellites are several orders lower again. For comparison with an experimental spectrum a knowledge of the initial hole state population distribution is required. This distribution will depend upon the nature of the ionizing probe and other experimental conditions.

4. Conclusions

For transitions which may be considered as formally involving only one electron, the dipole length and velocity forms of the transition moment appear to converge towards one another as the nuclear charge, or the principal quantum number of the Rydberg electron, is increased. This may be interpreted by examination of the

* Available from the authors on request.

generalized off-diagonal hypervirial theorem, which includes an expression which manifests differences in the initial and final state HF Hamiltonians, as an inequivalence in the alternative transition moment forms. Increasing Z or n diminishes the importance of electron repulsion effects, compared with nuclear Coulomb attraction in the initial and final states, thus making the HF Hamiltonians tend towards a single form.

Consideration of processes which formally involve two electrons has revealed that correlation differences, which are an unavoidable quantity in any independent particle treatment, lead to divergent transition moment behaviour as Z is increased. The approximate nature of the acceleration operator as used in this study prevents a systematic discussion of its associated transition moments, except the realization that the approximation $\nabla_\mu\{1/(\boldsymbol{r}_\mu - \boldsymbol{r}_{\mu'})\} = 0$ appears not to be severe. It is clear from the above that the use of any single form of the transition moment is insufficient to determine a transition probability within the relaxed HF formalism. Experimental X-ray intensity data are required to clarify if either the length or velocity form is able to provide reasonable theoretical predictions, especially in the case of processes which may be considered as single particle dipole transitions. It seems likely that a relaxed HF treatment is not appropriate for cooperative two particle transitions of the types considered. The assumption that negligible correlation differences exist between initial and final state wavefunctions in these cases is not justified, and leads to difficulties in the evaluation of radiative transition probabilities, where a wide spread of values is encountered between the dipole forms.

References

Ågren, H., Nordgren, J., Selander, L., Nordling, C., and Siegbahn, K. (1978). *J. Electron Spectrosc. Relat. Phenom.* **14**, 27.
Best, P. E. (1974). 'X-Ray Spectroscopy' (McGraw–Hill: New York).
Cohen, M., and MacEachran, R. P. (1972). *Chem. Phys. Lett.* **14**, 207.
Dyall, K. G. (1980). Ph.D. Thesis, Monash University.
Dyall, K. G., and Larkins, F. P. (1982). *J. Phys.* B **15**, 1811.
Grant, I. P. (1974). *J. Phys.* B **7**, 1458.
Grant, I. P., and Starace, A. F. (1975). *J. Phys.* B **8**, 1999.
Hansen, A. E. (1967). *Mol. Phys.* **13**, 425.
Larkins, F. P. (1971). *J. Phys.* B **4**, 1.
Löwdin, P. O. (1955). *Phys. Rev.* **97**, 1490.
Manson, S. T. (1976). *Adv. Electron. Electron Phys.* **41**, 73.
Mayers, D. F., and O'Brien, M. (1968). *J. Phys.* **1**, 145.
Nordgren, J., Ågren, H., Nordling, C., and Siegbahn, K. (1979). *Phys. Scripta* **19**, 5.
Nordling, C. (1982). Proc. AIP Conf., Univ. of Oregon, Vol. 94 (Ed. B. Crasemann), p. 415 (AIP : New York).
Starace, A. F. (1971). *Phys. Rev.* A **3**, 1242.
Starace, A. F. (1973). *Phys. Rev.* A **8**, 1142.

Manuscript received 6 July, accepted 10 October 1983